International Journal of Environment, Agriculture and Biotechnology
Vol-10, Issue-2; Mar-Apr, 2025
Peer-Reviewed International Journal
Journal Home Page Available: https://ijeab.com/
Journal DOI: 10.22161/ijeab

Teleconnection between Atmospheric Circulation and Meteorological Drought in Southwest China

Lirong Xu, Xiaoyuan Cheng, Guangxing Huang, Xuantao Liu, Haoxian Liang, Ruei-Yuan Wang*

School of Sciences, Guangdong University of Petrochem Technology (GDUPT), Maoming 525000, China
*Corresponding author: Ruei-Yuan Wang

Received: 28 Feb 2025; Received in revised form: 27 Mar 2025; Accepted: 02 Apr 2025; Available online: 07 Apr 2025

Abstract— *Meteorological drought represents one of the most prevalent and consequential climate disasters in China, exerting severe impacts on regional ecosystems and socioeconomic development. This study investigates the teleconnection between meteorological drought and atmospheric circulation patterns in Southwest China from 1960 to 2022. Employing the Standardized Precipitation Evapotranspiration Index (SPEI) across multiple temporal scales alongside atmospheric circulation data, we conducted a comprehensive analysis using statistical methodologies including run theory, Mann-Kendall trend tests, and Pearson correlation analysis. These approaches enabled an in-depth examination of the spatiotemporal characteristics of drought events and their atmospheric teleconnections in the region. The results demonstrate that (1) Since 1960, the seasonal drought occurrence probability in Southwest China follows the order: spring > winter > autumn > summer. Light and moderate droughts are the predominant types in the study area, while severe droughts occur relatively infrequently, with no extreme drought events recorded. (2) Significant spatial variations in meteorological drought exist at seasonal scales across Southwest China. Spring drought generally shows a mitigation trend, summer exhibits a northeast-wet/southwest-dry pattern, autumn demonstrates increasing aridity in most regions, and winter displays a distinct southeast-wet/ central-dry/ northwest-wet gradient. (3) Regional atmospheric circulation influences exhibit distinct patterns: ENSO demonstrates the most pronounced teleconnection impact across the entire region; PDO shows strong secondary influence, particularly in southeastern and northern areas; AO exhibits relatively weak effects, mainly affecting northern and northwestern sectors; and NAO displays minimal impact, with only 7.1% of southern and northern areas showing significant positive correlations. These findings provide valuable scientific references for drought research and integrated management in Southwest China, offering both theoretical foundations and empirical support for regional economic development planning. The results contribute to enhanced drought monitoring systems and informed policymaking for climate adaptation strategies in the region.*

Keywords— ***Southwest China; Meteorological drought; Atmospheric circulation; Standardized Precipitation Evapotranspiration Index (SPEI); Teleconnection***

I. INTRODUCTION

Drought, characterized by its cyclical recurrence, extensive spatial coverage, prolonged duration, and substantial economic impacts [1], represents one of the most economically consequential meteorological disasters among natural hazards [2]. This phenomenon typically induces cascading natural and socioeconomic consequences, including agricultural yield reduction, food security threats, ecosystem degradation, and regional gross domestic product (GDP) decline [3, 4]. A representative case is the 2022 extreme drought event in the Yangtze River Basin, which at its peak affected approximately 6.632 million hectares (≈66,320 km²) of arable land, caused critical water source depletion, and created drinking water shortages for approximately 4.99 million people and 920,000 livestock [5]. These events significantly impaired socioeconomic development across the Yangtze Economic Belt.

Atmospheric circulation constitutes a fundamental component of Earth's climate system, whose anomalies and long-term variations exert critical influences on drought genesis, persistence, and intensity. Large-scale circulation modes, including the El Niño-Southern Oscillation (ENSO), Pacific Decadal Oscillation (PDO), North Atlantic Oscillation (NAO), and Arctic Oscillation (AO), serve as dominant regulatory signals governing global climate variability. These circulation systems exhibit three defining characteristics: significant periodicity (ENSO has a period of 2 to 7 years, and PDO has a period of 20 to 30 years); prominent signal persistence, which can be maintained for months to decades through air-sea coupling; strong predictability; and based on quantifiable indicators such as sea surface temperature (SST) and the pressure field (such as the Southern Oscillation Index), the prediction window can reach 6 to 12 months (especially significant for ENSO) [6]. Contemporary research has significantly advanced our understanding of drought-driving mechanisms via circulation indices, spatiotemporal drought pattern forecasting, and cross-scale teleconnection effects. These investigations have been systematically conducted across multiple spatial domains, encompassing watershed, regional, national, and global scales [7-9].

In drought research, scholars have employed diverse methodological approaches to quantify drought characteristics from multiple perspectives. Meteorological station data-derived drought indices constitute the predominant analytical framework, with several widely utilized metrics including the Standardized Precipitation Index (SPI), Palmer Drought Severity Index (PDSI), Composite Meteorological Drought Index (CI), and Relative Moisture Index (MI). Notable applications include Wang et al., who investigated multi-scale relationships between meteorological drought and soil moisture across China using SPI and MI [10]; Zhang et al., who analyzed spatiotemporal variations of seasonal wet/dry patterns in Northwest China through PDSI [11]; and Zhang et al., who conducted spatiotemporal characterization of 50-year drought features in Gansu's Loess Plateau employing CI [12]. Recent years have witnessed increasing scholarly attention to the Standardized Precipitation Evapotranspiration Index (SPEI) for drought assessment [13-15]. This index demonstrates particular utility for arid/semi-arid regions through its integrative consideration of temperature, precipitation, and evapotranspiration parameters, thereby providing a more comprehensive framework for drought monitoring and evaluation.

The western region of Southwest China exhibits a natural predisposition to aridity, resulting from the synergistic interplay of the Tibetan Plateau's orographic barrier, monsoon system instability, karst-dominated permeable topography, and anthropogenic influences. Systematic monitoring and mechanistic investigation of these factors will facilitate evidence-based policymaking for drought mitigation strategies.

II. THE STUDY AREA AND DATA SOURCES

2.1 The Study Area

Southwest China is geographically situated in the southwestern part of the country (20°54'–34°19'N, 97°21'–112°04'E), encompassing five provincial-level administrative units: Sichuan, Yunnan, and Guizhou provinces; Guangxi Zhuang Autonomous Region; and Chongqing Municipality (Figure 1). The Tropic of Cancer traverses this region, which shares borders with Central China to the east, Northwest China to the north, Vietnam

and Laos to the south, and the Tibet Autonomous Region and Myanmar to the west. The region spans a total area of 1,376,300 square kilometers, accounting for approximately 14.33% of China's total land area.

The topography of Southwest China exhibits remarkable diversity, characterized predominantly by plateaus, mountains, and hills that extend across three distinct topographic terraces. A pronounced northwest-to-southeast elevation gradient is observed, with higher altitudes in the northwestern sectors gradually decreasing towards the southeast. Climatically, the region falls primarily within the subtropical monsoon zone, featuring synchronous patterns of temperature and precipitation. Summers are typically hot and humid with abundant rainfall, while winters remain relatively mild and dry. Significant altitudinal variations across the region contribute to substantial spatial heterogeneity in climatic conditions. Which annual mean temperatures range from -2.8°C to 23.9°C, while total annual precipitation varies considerably between 54.6 mm and 2,675.6 mm. The mean annual relative humidity exhibits a similarly wide range, fluctuating from 46.6% to 85.0% across different locations. These pronounced gradients in temperature and precipitation reflect the complex interplay between monsoonal circulation patterns and the region's diverse topographic features.

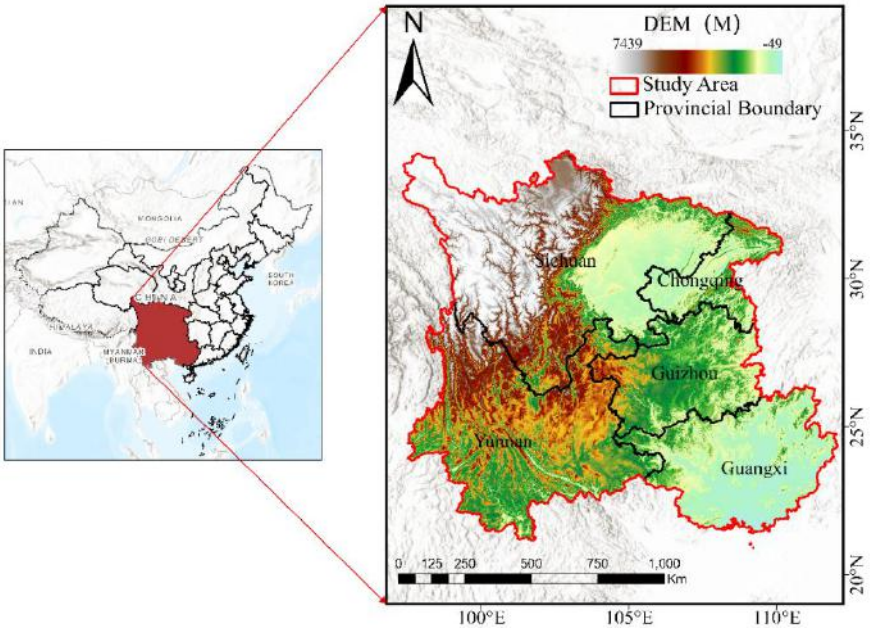

Fig.1 Map of the study area

2.2 Data Sources

SPEI data spanning 1960 to 2022 used in this study were obtained from the Software Engineering and Information Systems Institute (SEPI) created by the Consejo Superior de Investigaciones Ciengificas (Spanish National Research Council) (CSIC) (https://spei.csic.es/index.html). The atmospheric circulation indices employed in this research, including the North Atlantic Oscillation (NAO), Pacific-North American pattern (PNA), Arctic Oscillation (AO), Pacific Decadal Oscillation (PDO), and Southern Oscillation Index (SOI), were all acquired from the Earth System Research Laboratory (ESRL) of the National Oceanic and Atmospheric Administration (NOAA) (https://www.esrl.noaa.gov). These indices cover the same temporal period from 1960 to 2022 to ensure temporal consistency across all datasets.

III. METHODOLOGY

3.1 Material Processing Methods

3.1.1 The Standardized Precipitation-Evapotranspiration Index (SPEI)

SPEI, developed by Vicente-Serrano et al. [16], represents a multi-scalar drought index derived from the original SPI framework. This metric effectively captures regional drought conditions by incorporating both

precipitation and temperature influences while accounting for evapotranspiration effects. The computational procedure involves four sequential steps:

First, monthly potential evapotranspiration (PET) is calculated using the Thorn-thwaite method [17]:

$$PET = 16K(\frac{10T_i}{I})^m \quad (1)$$

$$m = 6.75 \times 10 - 7I3 - 7.71 \times 10 - 5I2 + 1.79 \times 10 - 2I + 0.492 \quad (2)$$

Here, PET denotes potential evapotranspiration (mm), Ti represents mean temperature (°C), K is a latitude and month dependent correction coefficient, I signifies the annual heat index (sum of 12 monthly heat indices), and m is a coefficient determined by I.

Second, the monthly climatic water balance (Di) is computed as the difference between precipitation (Pi) and PET:

$$D_i = P_i - PET_i \quad (3)$$

Third, the Di series undergoes probability distribution fitting using a three-parameter log-logistic distribution with the probability density function:

$$f(x) = \frac{\beta}{\alpha}\left(\frac{x-\gamma}{\alpha}\right)[1 + (\frac{x-\gamma}{\alpha})]^{-2} \quad (4)$$

where α, β, and γ represent scale, shape, and location parameters, respectively. The cumulative distribution function F(x) is derived as:

$$F(x) = [1 + (\frac{\alpha}{x-\gamma})]^{-1} \quad (5)$$

Fourth, SPEI values are obtained through normal standardization of F(x) [18]:

For $P \leq 0.5$:

$$w = \sqrt{-2\ln(P)} \quad (6)$$

$$SPEI = w - \frac{C_0+C_1W+C_2W^2}{1+d_1W+d_2W^2+d_3W^3} \quad (7)$$

For $P > 0.5$:

$$SPEI = -\left(w - \frac{C_0+C_1W+C_2W^2}{1+d_1W+d_2W^2+d_3W^3}\right) \quad (8)$$

where C0 = 2.5155, C1 = 0.8028, C2 = 0.0103, d1 = 0.4327, d2 = 0.1892, and d3 = 0.0013.

Three temporal scales are commonly employed: SPEI-1 captures monthly drought variability, reflecting fine-scale drought processes; SPEI-3 characterizes seasonal drought patterns (spring: March-May, summer: June-August, autumn: September-November, winter: December-February) [19]; while SPEI-12 reveals inter-annual drought variations, effectively representing long-term drought trends. This multiscalar approach enables comprehensive drought assessment across different temporal dimensions, with each scale providing unique insights into drought evolution mechanisms.

This study investigates the spatiotemporal characteristics of meteorological drought and its teleconnections with atmospheric circulation patterns in Southwest China using the SPEI at 1, 3, and 12-month timescales. The analysis employs SPEI-12 and SPEI-3 to characterize drought variability across temporal and spatial dimensions, while SPEI-1 is utilized for atmospheric circulation correlation analysis. Seasonal drought conditions are represented by specific monthly SPEI-3 values: April for spring, July for summer, October for autumn, and December for winter.

Drought severity is classified according to internationally recognized standards into five distinct categories based on SPEI threshold values (Table 1): no drought, mild drought, moderate drought, severe drought, and extreme drought. This classification system enables systematic quantification of drought intensity and facilitates comparative analysis of drought events across different temporal scales and geographical regions.

Table 1 SPEI drought grade

Grade	Drought Type	SPEI Value
1	No drought	-0.5≤SPEI
2	Mild drought	-1.0<SPEI≤-0.5
3	Moderate drought	-1.5<SPEI≤-1.0
4	Severe drought	-2.0<SPEI≤-1.5
5	Extreme drought	SPEI≤-2.0

The ENSO represents a naturally occurring ocean-atmosphere interaction phenomenon characterized by SST variations in the eastern and central equatorial Pacific. The SST anomalies in the tropical Pacific region (5°N-5°S, 170°W-120°W), known as the Niño 3.4 region, serve as one of the primary indicators for ENSO characterization. El Niño and the Southern Oscillation constitute distinct oceanic and atmospheric manifestations

of ENSO, respectively. As the most significant tropical air-sea interaction pattern, ENSO has become a crucial physical basis for short-term climate prediction.

The PDO indexes SST variations in the North Pacific poleward of 20°N, exhibiting periodicities of 5-30 years. The PDO's influence on precipitation distribution resembles that of ENSO patterns.

The NAO emerges as the dominant mode of winter surface pressure variability in the North Atlantic/European sector of the Northern Hemisphere, serving as the primary atmospheric circulation pattern governing Mediterranean climate. The NAO demonstrates peak energy at approximately 7.3-year intervals.

The AO constitutes the fundamental mode of internal atmospheric dynamics in the Northern Hemisphere's extratropical regions, displaying an equivalent barotropic structure extending from the surface to the lower stratosphere. This hemispheric-scale variability pattern [20] exhibits characteristic spatial and temporal coherence across atmospheric levels.

3.2 Analysis Methods

3.2.1 Drought Feature Recognition–Runs Theory

This study employs an integrated approach combining the SPEI index with runs theory for drought identification, adopting K = -0.5 as the drought threshold [21]. In the time series analysis, consecutive periods where drought indices remain above a specified threshold are classified as positive runs, while those below constitute negative runs. Monthly SPEI values serve as the basis for drought determination, with SPEI < -0.5 indicating drought occurrence.

The application of runs theory to SPEI time series enables the extraction of key drought characteristics, including Duration: The temporal span from drought initiation to termination; Severity: Cumulative SPEI deficit during a drought event; Frequency: Total count of drought occurrences within the study period; Intensity: Average drought severity per unit time (severity/duration).

Three characteristic drought variables were derived from SPEI time series at 1, 3, and 12-month timescales. Drought events separated by a single time unit were merged to account for intermittent recovery periods. The drought event identification process based on runs theory is illustrated in Figure 2, demonstrating the methodology for quantifying drought parameters across multiple temporal scales. This approach facilitates comprehensive characterization of drought events while maintaining temporal resolution appropriate for both short-term and prolonged drought analysis.

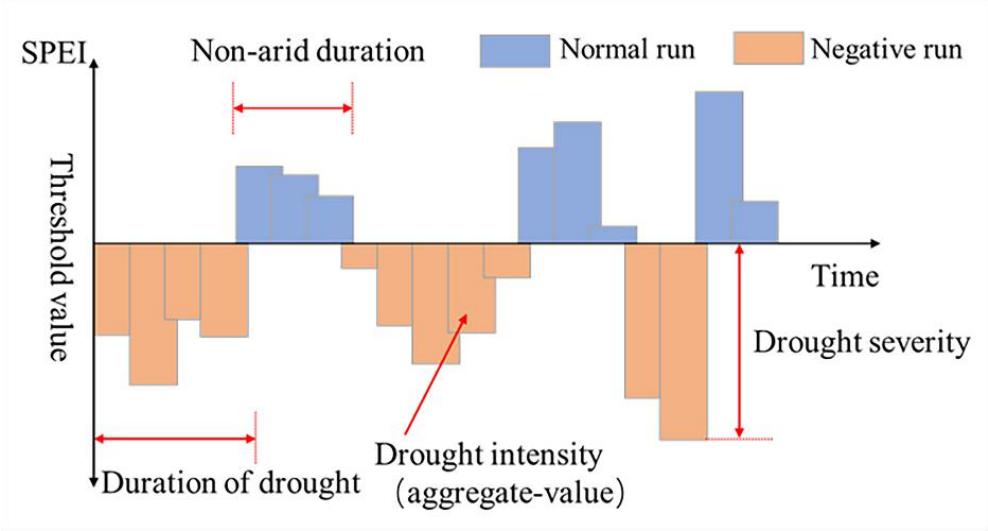

Fig.2 Identification of drought event process using runs theory

3.2.2 Trend Analysis and Detection

(1) Sen's Slope Estimator

The Theil-Sen Median method, commonly referred to as Sen's slope estimator, represents a robust non-parametric statistical approach for trend slope estimation, particularly advantageous when datasets

contain outliers or violate assumptions of conventional linear regression. This method requires no assumptions regarding underlying data distributions and derives the true slope as the median of all possible pairwise slopes within the time series, rendering it resistant to extreme values. Consequently, it has been widely adopted in meteorological, hydrological, and ecological studies involving long-term temporal analyses [22]. The computational formulation is expressed as:

$$\text{Slope} = Median(\frac{x_i - x_j}{i-j}) \quad (9)$$

where 1<j<i<n, with xi and xj denoting time series values at temporal points i and j, respectively, and Median representing the central tendency measure of the derived slopes.

Sen's slope estimator quantitatively characterizes the rate of temporal change within sequential data [23]. The interpretation criteria for slope magnitudes are presented in Table 2, facilitating standardized assessment of trend significance and directionality. This approach provides a distribution-free alternative to parametric trend analyses while maintaining robustness against non-Gaussian data distributions and measurement anomalies.

Table 2 Slope criteria

Slope value	Trend
Slope<0	Downward trend
Slope=0	Unchanged trend
Slope>0	Upward trend

(2) Mann-Kendall Trend Test

The Mann-Kendall (MK) trend test represents a non-parametric statistical method for detecting significant monotonic trends in time series data. This approach demonstrates particular robustness against outliers and requires no assumptions regarding data distribution, making it universally applicable to diverse datasets, including non-normally distributed and ordinal discrete variables. Widely adopted in climatological and hydrological studies [24], the method calculates test statistics through the following formulations: Test Statistic (S):

$$S = \sum_{k=1}^{n-1} \sum_{j=k+1}^{n} Sgn(X_j - X_k) \quad (10)$$

where: Xj denotes the j-th data point in the time series; n represents the sample size; The *sgn* function *sgn*(θ) is defined as:

$$sgn(\theta) = \begin{cases} +1 & (\theta > 0) \\ 0 & (\theta = 0) \\ -1 & (\theta < 0) \end{cases} \quad (11)$$

Standardized Test Statistic (Z):

$$Z = \begin{cases} \frac{(S-1)}{\sqrt{Var(S)}} & S > 0 \\ 0 & S = 0 \\ \frac{(S+1)}{\sqrt{Var(S)}} & S < 0 \end{cases} \quad (12)$$

where S follows a normal distribution with zero mean; Variance Var(S) = [n(n-1)(2n+5)]/18; Positive Z values indicate increasing trends, while negative values denote decreasing trends. Significance Thresholds: Trend significance is determined when |Z| exceeds critical values: 1.64 (90% confidence), 1.96 (95% confidence), and 2.58 (99% confidence) [25].

This study synergistically combines the Theil-Sen Median estimator for spatiotemporal drought characteristic analysis across Southwest China with the MK test to evaluate trend significance in SPEI data (1960–2022). The dual approach ensures robust quantification of trend magnitude (via Sen's slope) and statistical significance (via the MK test), providing comprehensive trend characterization. Detailed significance evaluation criteria are presented in Table 3.

Table 3 Significance detection criteria

Confidence standard Z	Significance level α	Significance
Z≤-2.58	α≤0.01	Extremely significant decline
-2.58≤Z≤-1.96	α≤0.05	Significant decline
-1.96≤Z≤1.64	α≤0.1	Unchanged
1.64≤Z≤1.96	α≤0.05	Significant rise
1.96≤Z≤2.58	α≤0.01	Extremely significant rise

3.2.3 Pearson Correlation Analysis

The Pearson correlation coefficient (PCC), also known as Pearson's product-moment correlation coefficient, is a statistical measure that quantifies the linear relationship between two variables. It is calculated as the covariance of the variables divided by the product of their standard deviations. The coefficient, denoted as r, ranges

between -1 and 1, where r < 0 indicates a negative correlation, r > 0 indicates a positive correlation, and values closer to |1| signify a stronger linear relationship [26]. In this study, Pearson correlation analysis was employed to quantitatively assess the relationship between SPEI and atmospheric circulation indices.

Given two samples, $X = (x_1, x_2, ..., x_n)$ and $Y = (y_1, y_2, ..., y_n)$, the Pearson correlation coefficient is computed as:

$$r = \frac{1}{n}\sum_{i=1}^{n}\left(\frac{x_i-\bar{x}}{\sigma_x}\right)\left(\frac{y_i-\bar{y}}{\sigma_y}\right) \quad (13)$$

where:

The significance of Pearson correlation coefficient is tested by t value test, in which the level of significance test is 0.05. When t is less than 0.05, it is significant, and t>=0.05 is not significant. The correlation formula is:

$$t = r\sqrt{\frac{n-2}{1-r^2}} \quad (14)$$

Where n is the number of samples, r is the correlation coefficient, and t is the test value. When the sample size n is larger, the correlation coefficient r reaching significant correlation is smaller, so when the sample size is larger, due to the difference of sample data, the correlation coefficient is generally not very high, but the significance test can consider that the correlation between the two groups of sample data is significant.

IV. RESULTS

4.1 Temporal Characteristics of Meteorological Drought

Analysis of the SPEI across multiple temporal scales provides critical insights into the dynamic evolution of hydrological processes, including precipitation and evapotranspiration patterns, over the study period. This study generated multi-scale SPEI time series (1-month, 3-month, and 12-month) for Southwest China from 1960 to 2022 (Figure 3), revealing distinct scale-dependent characteristics in drought variability.

The results show that there are significant differences in the sensitivity of the multi-time scale values of the SPEI in Southwest China to changes over time. The SPEI-1 time series exhibits a high degree of volatility, indicating that on a one-month time scale, the SPEI value is more sensitive to short-term climate changes. This high sensitivity suggests that SPEI-1 is more suitable to serve as a powerful tool for monitoring and assessing short-term climate anomaly events, such as extreme droughts or floods. Although the volatility of SPEI-3 remains relatively high, its changes are smoother compared to SPEI-1. This may be because on a three-month time scale, short-term meteorological changes are partially smoothed out, yet it can still reflect short-term or medium-term climate anomalies. The fluctuations in the SPEI-12 time series are significantly gentler, suggesting that on a 12-month time scale, the SPEI value responds more stably to climate changes. The long-term averaging effect reduces short-term fluctuations, making SPEI-12 more appropriate for evaluating long-term climate trends or predicting future climate changes.

It can be seen from the SPEI-12 time series graph that since 1960, there have been multiple obvious drought events in Southwest China, which demonstrates the frequent occurrence of droughts in this region. The obvious drought years in Southwest China include the period from spring 1960 to spring 1961, from autumn 1962 to spring 1964, from spring 1969 to spring 1970, from spring 1986 to spring 1990, from spring 2003 to spring 2008, and from spring 2009 to spring 2014. Some of these drought events had a relatively long duration, such as the periods from spring 1986 to spring 1990, from spring 2003 to spring 2008, and from spring 2009 to spring 2014. The results indicate that Southwest China experienced long-term droughts during these periods, which may have had long-term impacts on the local agriculture, water resources, and ecosystems.

International Journal of Environment, Agriculture and Biotechnology
Vol-10, Issue-2; Mar-Apr, 2025
Peer-Reviewed International Journal
Journal Home Page Available: https://ijeab.com/
Journal DOI: 10.22161/ijeab

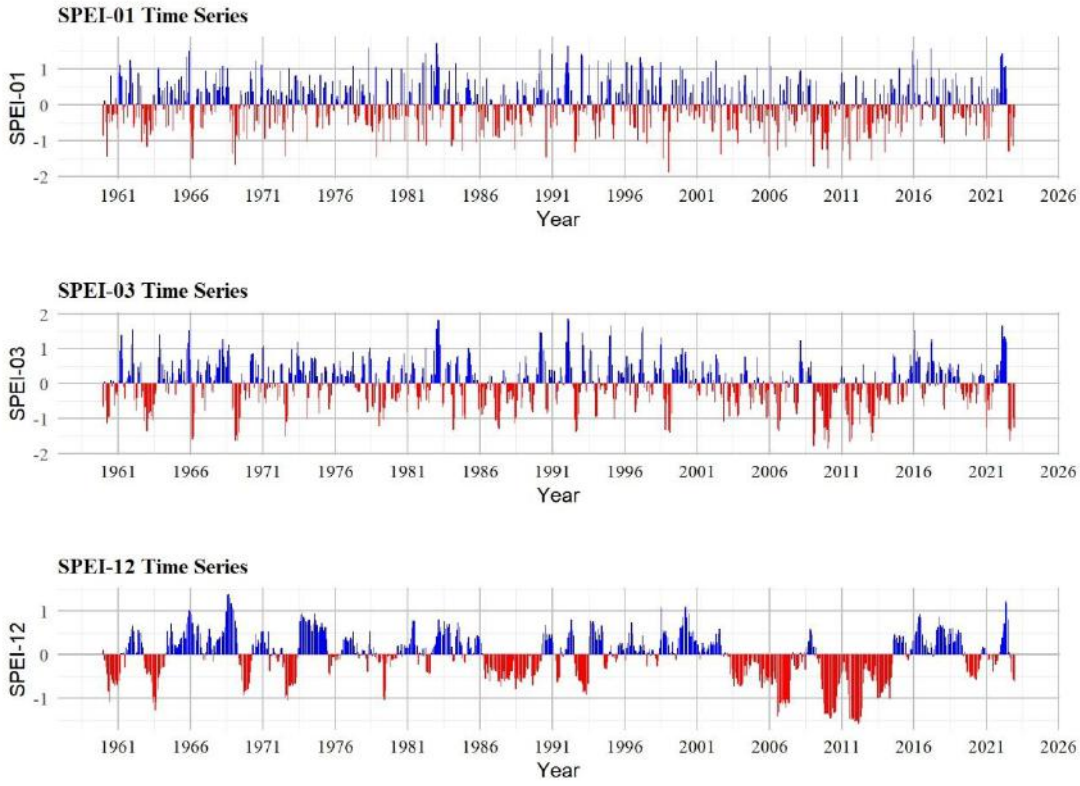

Fig.2 Multiscale time series from 1960-2022 in Southwest China

4.1.1 Temporal Characteristics of Drought Duration, Intensity, and Frequency

In assessing drought severity, both drought duration and intensity serve as critical evaluation criteria. This study employs runs theory to classify drought levels based on the SPEI, with a drought threshold set at k = −0.5. Statistical analyses were conducted on the annual and seasonal drought duration and intensity in Southwest China, with results presented in Figure 4.

As illustrated in Figure 4(a), the inter-annual analysis reveals that the maximum SPEI-based drought duration reached 21 months (2005–2007), with a minimum drought intensity of −1.31. Notably, a severe drought lasting five months (December 2011–April 2012) occurred in Southwest China, representing an extreme climatic event with profound environmental impacts. Additionally, frequent droughts were observed between 2002 and 2014, consistent with historical drought records in the region.

As shown in Figure 4(a), at the seasonal scale, the spring drought duration reached three months during the two consecutive years of 2009–2010. Similar three-month spring droughts were also recorded in 1960, 1963, 1966, 1969, 1979, and 1987. In summer, only the year 2011 experienced a drought lasting three months. Autumn droughts in 1992, 2003, 2009, and 2022 exhibited longer durations compared to other years, while winter droughts lasting three months occurred in 1962, 1968, 2010, and 2012.

Looking at Figure 4(b) reveals that the maximum SPEI-based drought intensity occurred in winter 2010, reaching −1.55. Additionally, the drought intensity in spring 1969 and winter 2010 fell below −1.50, classifying these years as severe drought events. Furthermore, the observational results from Figure 4 indicate a notable discrepancy between seasonal and inter-annual drought intensity, primarily attributable to differences in temporal scales and associated influencing factors. Seasonal drought intensity focuses on drought conditions within specific

seasons, closely linked to seasonal precipitation patterns, temperature fluctuations, and soil moisture levels. In contrast, inter-annual drought intensity encompasses drought conditions over an entire year, integrating drought severity across all seasons while accounting for the broader climatic influences. Consequently, inter-annual drought intensity tends to exhibit greater stability and is more susceptible to long-term climate change trends.

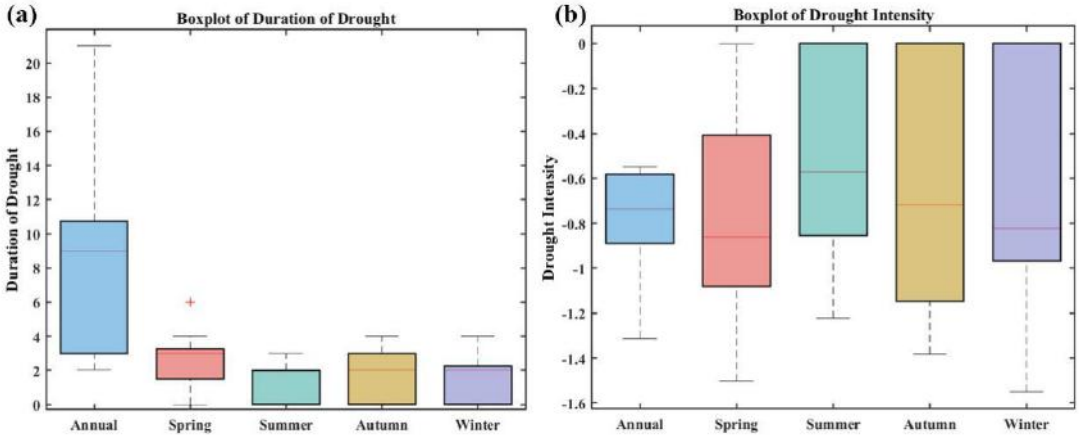

Fig.4 Seasonal characteristics of drought duration (a) and intensity (b) in Southwest China

Figure 5 presents the drought frequency statistics based on annual and seasonal SPEI drought classification standards, visualized through stacked bar charts. This representation enables observation of drought frequency distribution patterns in Southwest China at both inter-annual and seasonal scales. Comparative analysis of different drought severity categories reveals that mild and moderate droughts constitute the most prevalent drought types in the study region, whereas severe droughts occur relatively infrequently. Notably, extreme drought events were not observed at the inter-annual scale, as indicated by zero occurrence frequency.

Further examination of seasonal drought frequency demonstrates distinct patterns. Non-drought conditions exhibit their highest frequency during summer, likely attributable to increased precipitation in this season. Mild droughts emerge as the second most frequent category, peaking in spring with a frequency of 17.46% and reaching their lowest occurrence (11.11%) in summer. Moderate droughts show significant occurrence in autumn (7.41%) and winter (6.35%), with comparatively lower frequencies in other seasons. Severe droughts maintain consistently low frequencies across all seasons, though spring and winter share identical occurrence rates of 2.12%, exceeding those observed in summer and autumn.

The seasonal distribution of drought frequency demonstrates pronounced seasonal characteristics in Southwest China, following the hierarchical pattern: spring > winter > autumn > summer. This pattern suggests elevated drought risks during spring and winter, while summer presents the lowest drought risk due to abundant precipitation. These seasonal variations likely reflect regional climatic patterns and precipitation distribution, with higher drought frequencies in spring and winter potentially associated with reduced precipitation and specific climatic conditions characteristic of these seasons.

International Journal of Environment, Agriculture and Biotechnology
Vol-10, Issue-2; Mar-Apr, 2025
Peer-Reviewed International Journal
Journal Home Page Available: https://ijeab.com/
Journal DOI: 10.22161/ijeab

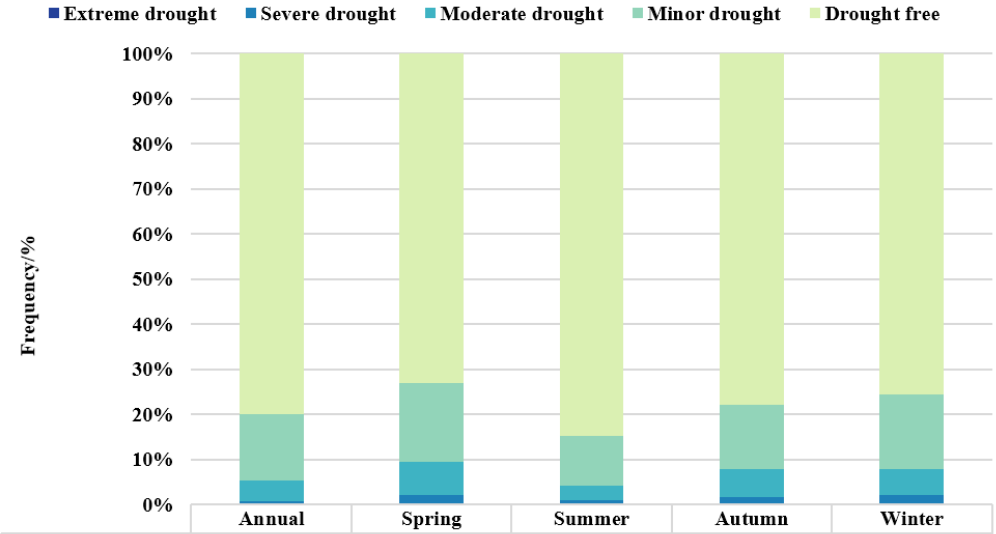

	Annual	Spring	Summer	Autumn	Winter
Drought free	79.89	73.02	84.66	77.78	75.66
Minor drought	14.68	17.46	11.11	14.29	16.4
Moderate drought	4.76	7.41	3.17	6.35	5.82
Severe drought	0.66	2.12	1.06	1.59	2.12
Extreme drought	0	0	0	0	0

Fig.5 Time variation of drought frequency at different levels in Southwest China

4.2 Spatial Variation Trends of Drought

This study conducted an in-depth analysis of the spatial characteristics of SPEI in Southwest China at the seasonal scale from 1960 to 2022 (Figure 6), yielding the following results:

Spring (Figure 6-a): Most regions in Southwest China exhibited a mitigation trend in meteorological drought. However, only northwestern Sichuan, Xishuangbanna in Yunnan, and southeastern Guizhou passed the significance level test. Specifically, the northwestern part of the Aba Tibetan and Qiang Autonomous Prefecture in Sichuan showed the most significant wetting trend (slope = 0.0047, $\alpha \leq 0.01$). Xishuangbanna in Yunnan reached a significance level of $\alpha \leq 0.05$, while southeastern Guizhou showed a weaker but still notable trend ($\alpha \leq 0.1$), indicating a more pronounced wetting tendency in these regions.

Summer (Figure 6-b): The drought-wetness trends in Southwest China displayed a distinct polarization. Most of the southwestern study area, particularly Lincang, Pu'er, Yuxi, and the Honghe Hani and Yi Autonomous Prefecture in Yunnan, exhibited a significant drying trend (minimum Sen slope = -0.0048, $\alpha \leq 0.01$). In contrast, the northeastern regions, especially Nanchong, Bazhong, Dazhou, and Guang'an in Sichuan, demonstrated a wetting trend (maximum Sen slope = 0.0042, $\alpha \leq 0.01$). This spatial divergence suggests contrasting climatic influences between the southwestern and northeastern parts of the study area during summer.

Autumn (Figure 6-c): Approximately 97.22% of the study area exhibited positive Sen's slope values, indicating a predominant drought intensification trend across Southwest China. Particularly significant drying trends ($\alpha \leq 0.01$) were observed in eastern Sichuan, Liupanshui, and southeastern Guizhou, as well as Baise City in Guangxi. The spatial pattern of significance levels revealed a concentric distribution centered around the tri-province border area, with decreasing significance levels (from 99% to 95% to 90%) extending toward the northern and eastern peripheries. The most pronounced drying occurred in Honghe Hani and Yi Autonomous Prefecture, Yunnan, with a minimum Sen's slope of -0.0052.

Winter (Figure 6-d): Meteorological drought trends displayed marked regional heterogeneity. Significant

drying trends ($\alpha \leq 0.01$) were evident in eastern Sichuan (Liangshan Yi Autonomous Prefecture, Leshan, and Yibin), with a minimum Sen's slope of -0.0069. Similar patterns were observed throughout most of Yunnan (western and northern regions) and Chongqing (except southeastern portions). Spatially, the winter drought trends followed a distinct southeast-central-northwest gradient, exhibiting a wet-dry-wet transitional pattern across the study area.

Spatiotemporal Synthesis: The analysis reveals pronounced seasonal and regional disparities in meteorological drought trends from 1960 to 2022. Spring was characterized by widespread drought mitigation across most regions. Summer exhibited a polarized northeast (wetting)-southwest (drying) dipole pattern. Autumn showed predominant drought intensification, particularly in eastern Yunnan ($\alpha \leq 0.01$). Winter displayed a tripartite spatial regime with alternating wet-dry-wet zones along the southeast-central-northwest axis. These patterns underscore the complex interplay of regional climate systems and topographic influences governing drought evolution in Southwest China.

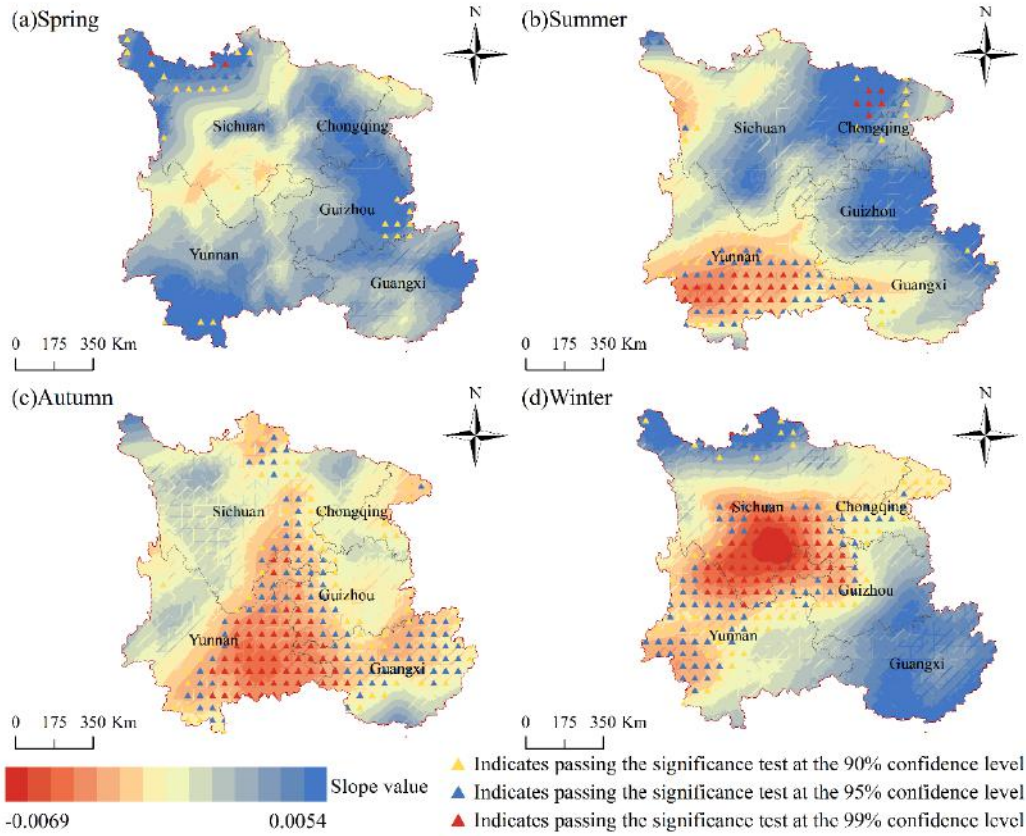

Fig.6 Spatial characteristics of seasonal scale meteorological drought in Southwest China from 1960-2022

4.3 Response of Meteorological Drought to Atmospheric Circulation

Using Pearson correlation analysis, we examined the relationship between drought indices and atmospheric circulation patterns, identifying key drought-influencing factors in Southwest China through significance testing (Table 4). The AO showed relatively weak correlations, with only 8.7% of the region exhibiting significant positive correlations and 1.1% showing significant negative correlations, primarily concentrated in the northwestern parts of Southwest China (Figure 7-a). The NAO demonstrated the lowest significance, with merely 7.1% positive correlations distributed along the northern and southern margins of the region (Figure 7-b). The ENSO exhibited the strongest statistical significance, indicating its dominant influence on drought patterns in Southwest China. Significant positive correlations covered 14.4% of the region, mainly in the southeastern areas, while negative

correlations accounted for 42.4%, predominantly distributed across northeastern and southwestern zones (Figure 7-c). The PDO showed the highest proportion of significant positive correlations (43.2%) among all indices, with negative correlations covering 10.1% of the region. Spatially, positive correlations clustered in eastern and partial northwestern areas, whereas negative correlations were concentrated in the northeastern sector (Figure 7-d).

Spatial analysis revealed distinct correlation patterns:

- AO-drought index correlations followed a north > central > south gradient (Figure 7-a).
- NAO's strongest influences appeared in southern and northern areas, particularly showing positive correlations in Aba Tibetan and Qiang Autonomous Prefecture (Sichuan) and Xishuangbanna Dai Autonomous Prefecture (Yunnan) and negative correlations in Laibin and Guigang (Guangxi) (Figure 7-b).
- ENSO correlations displayed a north > southeast > northwest > southwest hierarchy (Figure 7-c).
- PDO's strongest impacts occurred in southeastern and northern regions, with notable positive correlations in Guizhou and western Guangxi, and negative correlations in northern Aba Tibetan and Qiang Autonomous Prefecture (Sichuan).

These results demonstrate that AO, NAO, ENSO, and PDO primarily influence northern Southwest China, followed by southeastern and southern regions, revealing complex spatial variability in atmospheric circulation impacts on regional drought patterns.

Table 4 Significance of correlation between atmospheric circulation index and drought index (SPEI)

	AO	NAO	ENSO	PDO
Significant positive correlation	8.7%	7.1%	14.4%	43.2%
Significant negative correlation	1.1%	0	42.4%	10.1%
No significant correlation	90.2%	92.9%	43.2%	46.7%

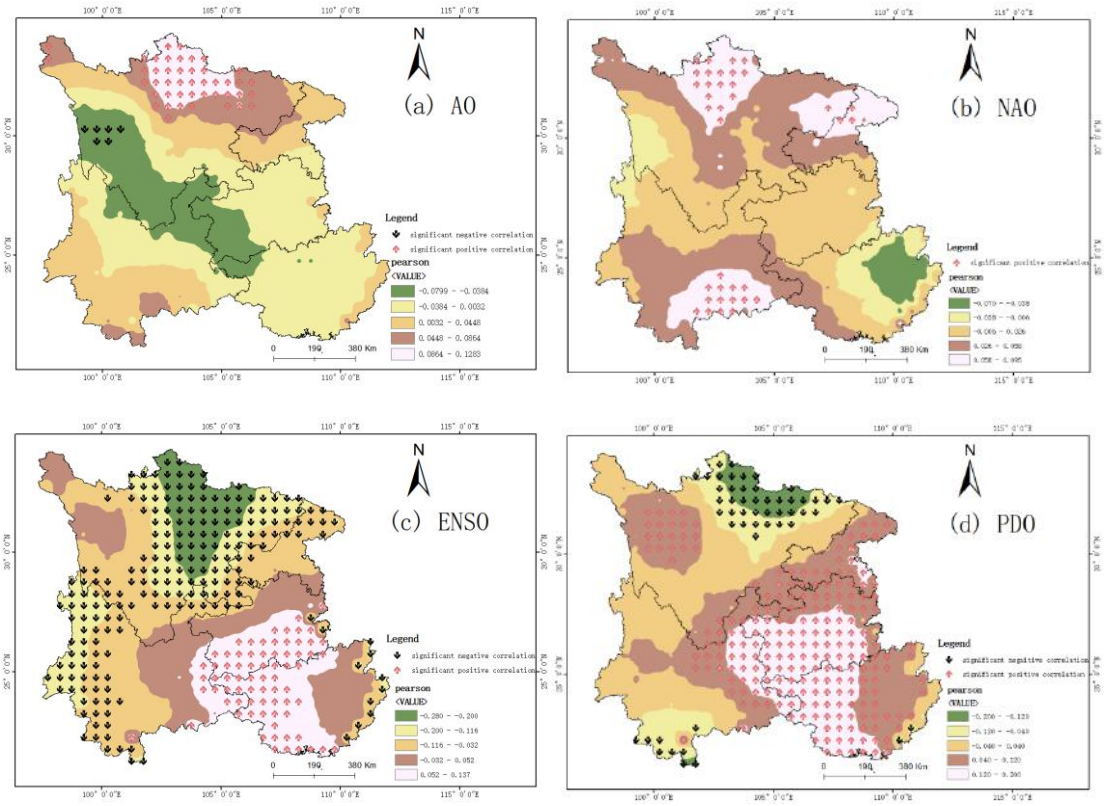

Fig.7 Spatial distribution of significant correlation between atmospheric circulation and drought index (SPEI) in Southwest China

International Journal of Environment, Agriculture and Biotechnology
Vol-10, Issue-2; Mar-Apr, 2025
Peer-Reviewed International Journal
Journal Home Page Available: https://ijeab.com/
Journal DOI: 10.22161/ijeab

V. DISCUSSION

5.1 Comparative Analysis of Meteorological Drought in Southwest China and Other Regions

This study systematically investigated the spatiotemporal characteristics of meteorological drought in Southwest China and its teleconnections with atmospheric circulation patterns, yielding robust conclusions. The results reveal significant seasonal disparities in drought occurrence frequencies, with spring and winter exhibiting higher drought frequencies compared to summer and autumn. Notably, substantial variations in drought evolution patterns persist even among adjacent regions [18, 27], suggesting that drought drivers may be closely associated with region-specific topographic features, climatic regimes, and anthropogenic activities [28].

Through comparative analysis of the relationships between key atmospheric circulation indices (AO, NAO, PDO, ENSO) and the SPEI drought index, this study demonstrates distinct differential impacts among various teleconnection factors. ENSO emerges as the most influential factor on drought conditions in Southwest China, while NAO shows the weakest correlation. These findings align with Xu et al. [29], who identified ENSO as the dominant influence on drought patterns across China. Consequently, ENSO could be effectively incorporated as an input parameter in drought early warning systems to enhance forecasting accuracy.

This research elucidates both the spatiotemporal characteristics of drought in Southwest China and its atmospheric circulation linkages. The findings establish a novel theoretical framework for understanding regional drought events, with significant implications for water resource management, agricultural planning, and ecological conservation. Particularly, the strong drought response to ENSO variations provides a scientific basis for climate prediction and drought early warning systems in the region. The identification of ENSO's predominant influence offers valuable insights for developing targeted drought mitigation strategies in this ecologically sensitive area.

This study has made significant progress in elucidating the spatiotemporal characteristics of meteorological drought in Southwest China and its teleconnections with atmospheric circulation patterns. However, several limitations warrant consideration for future research improvements.

The complex climatic heterogeneity of Southwest China, characterized by substantial elevational gradients and diverse natural conditions [30], presents challenges in drought assessment. While this research primarily focused on atmospheric circulation indices as drought drivers, it did not fully account for other potential contributing factors such as land-use changes and anthropogenic activities [31]. Future investigations should adopt a more comprehensive approach by integrating multiple influencing factors to better understand drought formation mechanisms and evolutionary processes.

Methodologically, this study was limited to assessing meteorological drought within the region, without extending the analysis to hydrological, agricultural, or socioeconomic drought impacts and their progression cycles. Although the SPEI demonstrated satisfactory applicability in characterizing meteorological drought events—showing good consistency with historical drought records in terms of timing and severity—the regional suitability of drought indices requires further validation [32]. The question of whether SPEI represents the optimal drought indicator for this specific region remains open for investigation. Future research directions should focus on developing integrated assessment frameworks incorporating multiple drought types. Validating and optimizing drought indices for regional specificity. Employing advanced climate models and statistical approaches to enhance drought prediction capabilities. These methodological advancements would significantly improve drought management strategies and climate change adaptation measures, not only for Southwest China but also for other drought-prone regions globally. The integration of multidisciplinary approaches will be crucial for addressing the complex challenges posed by drought under changing climatic conditions.

VI. CONCLUSION

This study employed the SPEI index at various temporal scales from 1960 to 2022 to analyze meteorological drought characteristics in Southwest China. Using runs theory, we conducted a detailed assessment of drought duration, intensity, and frequency, investigating the spatiotemporal evolution and trends of drought over the past 63 years. Additionally, we examined the teleconnections between meteorological drought and atmospheric circulation patterns to identify key influencing factors. The main conclusions are as follows:

(1) **Temporal Characteristics of Drought:**

At the inter-annual scale, the longest drought duration in Southwest China reached 21 months (2005–2007). Seasonally, the maximum SPEI-based drought intensity occurred in winter 2010, with spring 1969 and winter 2010 classified as severe drought years. Seasonal drought frequency analysis revealed a consistent hierarchy: spring > winter > autumn > summer. Mild and moderate droughts were the most common types, while severe droughts occurred less frequently, with no extreme drought events recorded.

(2) Spatial Variability of Drought Trends:

Significant spatial heterogeneity was observed in seasonal drought patterns:

Spring: Overall drought mitigation trend.

Summer: A distinct northeast (wetting)-southwest (drying) dipole pattern.

Autumn: Predominant intensification of drought across most regions.

Winter: A tripartite spatial regime with wet-dry-wet transitions from southeast to central to northwest regions.

(3) **Influence of Atmospheric Circulation Patterns:**

Regional drought responses to atmospheric circulation exhibited marked variability: **ENSO** exerted the strongest influence, with significant correlations across 56.8% of the study area. **PDO** showed the second-highest impact (53.3% significant correlations), primarily affecting southeastern and northern regions. **AO** demonstrated weaker drought associations, limited to northern and northwestern areas. **NAO** had the least influence, with only 7.1% of the region (northern and southern margins) showing significant positive correlations.

These findings enhance our understanding of drought mechanisms in Southwest China, providing a scientific basis for drought prediction, water resource management, and climate adaptation strategies. Future research should further explore the combined effects of multiple climatic drivers and regional-scale anthropogenic influences on drought variability.

ACKNOWLEDGEMENTS

This research is supported by the Innovation and Entrepreneurship Training Program Fund for College Students of GDUPT (Project No. 24C201), as part of the ongoing study on Multi-angle analysis and driving mechanism of meteorological conditions on surface vegetation in Southwest China.

REFERENCES

[1] Zhang, Q.， Yao, Y.， Li, Y.， Huang, J.， Ma, Z.， Wang, Z.， Wang, S.， Wang, Y.， and Zhang, Y. 2020. Progress and prospect on the study of causes and variation regularity of droughts in China. Acta Meteorologica Sinica，2020, 78(3): 500-521. DOI:10.11676/qxxb2020.032.

[2] Shi, P., Tang, H., and Qu, S. Characteristics of propagation from meteorological drought to hydrological drought in Southwest China. Water Resources Protection, 2023, 39(1):49-56.

[3] Deng, H. Impact of meteorological disasters on macadamia nut production in Yongde County and its prevention strategies Southern agriculture, 2025, 19 (01): 217-219.

[4] Park, S., Zhang, X., Chen, A., Liu, Q., Lian, X., Wang, X., Peng, S., and Wu, X. Impacts of extreme climate events on the carbon cycle of terrestrial ecosystems. Chinese Science: Geosciences, 2019, 49 (09): 1321-1334

[5] Xia, J., Chen, J., and She, D. Extreme drought events in the Yangtze River Basin in 2022 and their impacts and countermeasures. Journal of water conservancy, 2022.53 (10): 1143-1153. Doi: 10.13243/j.cnki. Slxb. 20220730

[6] Fan, L., Lu, A., and Zhang, W. Temporal and spatial characteristics of drought in Qinghai Province and its response to atmospheric circulation. Resources and environment in arid areas, 2021.35 (12): 60-65. Doi: 10.13448/j.cnki. Jalre. 2021.326

[7] Zou, D., Zhou, Y., Dong, X., Lin, J., Wang, H., and Liang, J. Spatiotemporal Association and Attribution Analysis of Vegetation and Drought in the Yangtze River Basin. Remote

Sensing Technology and Application, 2024, 39(5): 1183-1195

[8]Chen, Y., Zhao, Q., and Ai, M. Spatio-temporal characteristics of meteorological drought in the Liaohe River Basin from 1959 to 2019. Water Resources and Hydropower Engineering, 2023, 54(01):42-52.DOI:10.13928/j.cnki.wrahe.2023.01.004.

[9]Cao, Q., Liu, K., and Hao, Z. Analysis on drought mutation characteristic and its teleconnection factors in Songhua River Basin. YANGTZE RIVER, 2023, 54(12): 89-95.

[10]Wang, S., Zhang, C., Song, L., Li, Y., Feng, J., and Wang, J. Relationship Between Soil Relative Humidity and the Multiscale Meteorological Drought Indexes. Journal of Glaciology and Geocryology, 2013, 35(4):865-873.

[11]Zhang, Y., Chen, F., Gou, X., Jin, L., Tian, Q., Wang, Y., and Peng, J. The Temporal and Spatial Distribution of Seasonal Dry- Wet Changes over the Northwestern China: Based on PDSI. Acta Geographica Sinica, 2007, 62(11): 1142-1152 https://doi.org/10.11821/xb200711003.

[12]Zhang, T., Zhang, B., Wang, X., Jia, J., Yin, H., and He, X. Temporal and spatial analysis of drought for recent 50 years in Loess Plateau of Gansu province based on meteorological drought composite index. Ecology and Environment, 2012, 21(1): 13-20.

[13]Xue, H., Li, Y., and Dong, G. Analysis of Spatial-temporal Variation Characteristics of Meteorological Drought in the Hexi Corridor Based on SPEI Index. Chinese Journal of Agrometeorology, 2022, 43(11): 923-934.

[14]Cao, Y., Li, K., and Ren, Bl. Characteristics and driving factors analysis of meteorological drought in Liaoning Province based on SPEI. Advances in Science and Technology of Water Resources, 2022,42(5):28-36.

[15]Chen, Y., Zhang, Q., and Lyu, H. Study on temporal and spatial characteristics of meteorological drought in Huaibei Area Based on spei index. Journal of irrigation and drainage, 2024, 43(2):67-77.

[16]Vicente-Serrano, M. S., Beguería,. A Multiscalar Drought Index Sensitive to Global Warming: The Standardized Precipitation Evapotranspiration Index. Journal of Climate, 2010, 23 (7): 1696-1710, 1712, 1714-1718.

[17]Zhang, X., Wang, R., and Shan, F. Temporal and spatial distribution characteristics of drought in the three northeastern provinces from 1961 to 2020. Journal of irrigation and drainage, 2024, 43(1):78-88.

[18] Lu, J., Gan, R., Yang, F., and Zuo, Q. Drought Characteristics and Its Correlation with Circulation Index in Henan Province Based on SPEI Index. China Rural Water and Hydropower, 2022(4): 17-24.

[19] Liu, Z., Sun, Q., and Lu, H. Temporal and Spatial Characteristics of Droughts and Their Responses to Atmospheric Circulation in Ningxia. Research of Soil and Water Conservation, 2023, 30(03):225-231,239.

[20] Lee, C.W. Model and prediction of plant response to climate change based on sunlight induced chlorophyll fluorescence. Jiangnan University, 2023. Doi: 10.27169/d.cnki. Gwqgu. 2023. 001714

[21] Hu, X. Temporal and spatial evolution and prediction of meteorological drought in different climate regions of Gansu Province. Northwest University of agriculture and forestry science and technology, 2023. Doi: 10.27409/d.cnki. Gxbnu. 2023. 000876

[22] Ye, Z., Ye, X., and Li, Z. Evaluation of long-term temporal and spatial trend changes of long-term river flow in Taiwan by Mann Kendall and Theil Sen tests. Proceedings of the annual meeting and Symposium of the Chinese Society for soil and water conservation in 2015, 2015: 1-14

[23] Han, Z. Temporal and spatial evolution characteristics and transmission process of multi type drought in China. Xi'an University of technology, 2022. Doi: 10.27398/d.cnki. Gxalu. 2022. 001707

[24] Xia, M. Temporal and spatial evolution characteristics and cause analysis of meteorological drought in Huaihe River Basin. Anhui Normal University, 2020. Doi: 10.26920/d.cnki. Gansu.2020.000113

[25]Li, T., Lv, A., and Zhang, W. Spatiotemporal Characteristics of Watershed Warming and Wetting: The Response to Atmospheric Circulation in Arid Areas of Northwest China. Atmosphere, 2023b, 14(1):151-151.

[26]Zhang, L., Wang, H., and Gu, K. Research on Passenger Volume Prediction Model of Transportation Hub Station Based on Pearson Correlation Analysis. Communications Science and Technology Heilongjiang, 2023, 46(03): 137-139. DOI:10.16402/j.cnki.issn1008-3383.2023.03.030.

[27] Lyu, P., Zhou, Q., and Xian, J. Temporal and spatial characteristics of seasonal drought and its response to atmospheric circulation in Anhui Province. Water Resources and Hydropower Engineering, 2023, 54(12):93-105. DOI:10.13928/j.cnki.wrahe.2023.12.008.

[28] Liu, Z. Temporal and spatial changes and influencing factors of seasonal meteorological drought in Dongting Lake Basin.

Hunan Normal University, 2021. Doi: 10.27137/d.cnki. Ghusu.2021. 002685

[29]Xu, M., Wang, F., Xu, F. and Jia, M. Study on Drought Evolution Characteristics and Teleconnection Driving Forces Based on Vegetation Condition Index in China.Water Resources and Power,2024,v.42;No.284(04):20-24+19.

[30] Fan, L. Temporal and spatial pattern of drought in the Lancang Mekong basin and its relationship with atmospheric circulation response. Yunnan Normal University, 2022. Doi: 10.27459/d.cnki. Gynfc.2022. 001147

[31]Zhang, Q., Yao, Y., and Li, Y. Progress and prospect on the study of causes and variation regularity of droughts in China. Acta Meteorologica Sinica, 2020, 78(3):500-521.

[32] Xu, Z. Temporal and spatial variation characteristics of vegetation in Shandong Province and its response to meteorological drought index. Shandong Normal University, 2019.